16th Australasian Fluid Mechanics Conference
Crown Plaza, Gold Coast, Australia
2-7 December 2007

Computational Fluid Dynamics Modelling of Natural Convection in Copper Electrorefining

M.J Leahy and M.P. Schwarz
CSIRO Minerals, Clayton, Victoria, 3168 AUSTRALIA

Abstract

A computational fluid dynamics (CFD) model of copper electrorefining is discussed. Copper electrorefining takes place in a rectangular geometry, with two electrodes opposing each other, and a source and sink of copper ions at the respective electrodes. The resultant gradients in the copper concentration lead to buoyancy forces, and natural convection develops. The transport of copper ions is coupled to the Navier-Stokes equations in a CFD software package ANSYS CFX (version 11). Validation of the CFD model is provided for several cases varying in size, from a small laboratory scale to large industrial scale, including one that has not been compared with a CFD model previously. The larger scale systems are analysed in terms of the Rayleigh number, and we clarify that the important length scale for turbulence onset is the width of the cell, in addition to the cell height. Clarification of the appropriate turbulence model is given.

Introduction

Copper plate electrorefining (ER) is a process used in industry for refining copper. Copper is dissolved from the anode plate into solution and is plated onto the opposing cathode, by means of the passage of current between the plates. Natural convection is well known to develop is these ER systems, as has been investigated on small scale laboratory systems as discussed by Eklund et al [3], with experimental validation of CFD models, and in the context of larger systems in Denpo et al [2] and Gurniki et al [5]. The large scale systems have been thought to be turbulent, with a k-ε turbulence model used in the CFD modelling by Gurniki et al [5] of an experimental setup of Ziegler [7]. In this work we develop a similar CFD model and compare the results with the experimental setup of Ziegler [7], and investigate the appropriate turbulence model, and indeed the necessity of a turbulence model at all. We also compare the CFD model to experimental data [6] from a much larger system, which has not previously been used for comparison with a CFD model.

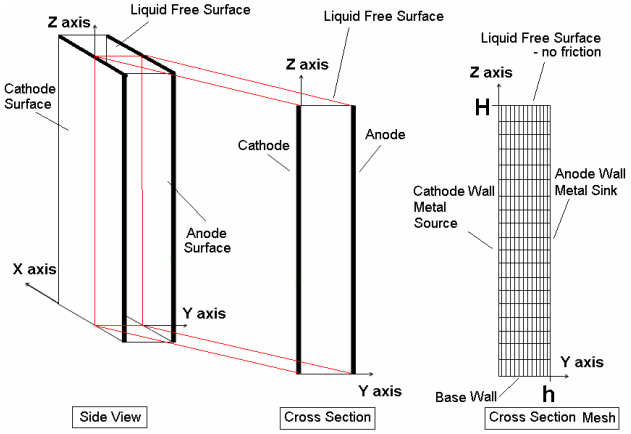

Figure 1. Schematic geometry, side and cross section views and cross section schematic mesh view on right. Actual mesh is not shown.

CFD Model

The CFD model is two-dimensional (2D) in a cross section of the cell, as shown in figure 1, with the assumption that the flow is negligible in the third dimension (X direction), parallel to the electrodes. The CFD model is set up within the ANSYS CFX framework [1]. The ER model is a single phase model which solves the Navier-Stokes equations, with an additional body force term to account for the buoyancy forces. A transport equation is solved for the concentration of the copper species (or other metal), with a source/sink at the appropriate anode and cathode boundary, based on Faraday's Law. The equation of continuity is given by

$$\nabla \cdot (\rho \mathbf{v}) = 0 \tag{1}$$

and the momentum equation in steady state is given by

$$\nabla \cdot (\rho \mathbf{v}\mathbf{v}) = -\nabla p' + \nabla \cdot [(\mu + \mu_T)(\nabla \mathbf{v} + \nabla \mathbf{v}^T)] + \mathbf{B} \tag{2}$$

where ρ is the electrolyte density (assumed constant), $\mathbf{v}$ is the velocity, p' is the (modified) pressure (including the hydrostatic part $-\rho \mathbf{g}.\mathbf{x}$), and $\mathbf{B}$ is the natural convection buoyancy force, described below. The laminar viscosity is denoted μ (kg m^{-1} s^{-1}), and μ_T (kg m^{-1} s^{-1}) is the turbulent viscosity, described in equation (5). The buoyancy body force is given by

$$\mathbf{B} = -\rho \mathbf{g} \beta (C - C_{ref}) \tag{3}$$

where $\mathbf{g}$ (m s^{-2}) is the gravity vector, C (g L^{-1}) is the concentration of copper, C_{ref} (g L^{-1}) is the average concentration of copper over the cathode, and β (L g^{-1}) is the coefficient of expansion for the copper species. The steady state transport equation for the copper species is given by

$$\nabla \cdot (C\mathbf{v}) = \nabla \cdot [(\rho D + \frac{\mu_T}{\sigma_T}) \nabla (\frac{C}{\rho})] + S^C \tag{4}$$

Where σ_T (-) is the turbulence Schmidt number taken as 0.9, S^C (g L^{-1} s^{-1}) is the source term, which describes the flux of copper at the anode and cathode, and D (m^2 s^{-1}) is the diffusion coefficient of copper (or other metal species).

The turbulent viscosity μ_T in equations (2) and (4) is determined by solving transport equations for the turbulence model, i.e. k-ε or k-ω. In this work both models were tested, and the k-ω was found to have the best close-to-wall behaviour (good velocity profile prediction). The turbulent viscosity can be written in terms of the transported variables - kinetic energy k (m^2 s^{-2}) and eddy frequency ω (s^{-1}) (or eddy dissipation if using k-ε) as

$$\mu_T = \rho \frac{k}{\omega} \tag{5}$$

Boundary Conditions

The boundary conditions for the flux of copper at the anode and cathode walls $\dot{m}_{copper}$ (kg m^{-2} s^{-1}) are based on Faraday's Law as follows:

$$\dot{m}_{copper} = \frac{(1 - t_+) i}{zF} \frac{M_{Cu}}{1000} \tag{6}$$

where i (A m^{-2}) is the current density, t_+ (-) is the transport number, F (A s mol^{-1}) is Faraday's constant, z (-) the valency, and M_{Cu} (g/mol) is the molecular weight of copper. On the anode side a positive flux is applied, whilst on the cathode a negative flux of same size is applied. At all walls, no slip boundary conditions are applied, whilst at the top free surface a free slip (no friction) boundary condition is applied.

Parameter	Eklund	Ziegler	Konishi
Current Density i (A m^{-2})	45.9	100	100
Temperature (^{o}C)	25	23	25
Liquid laminar viscosity μ (kg m^{-1} s^{-1})	0.9612 x10^{-3}	1.91 x10^{-3}	0.9612 x10^{-3}
Liquid Density ρ (g L^{-1})	1045.4	1200	1045.4
Coefficient of Expansion β (L g^{-1} s^{-1})	0.0022	0.00159	0.0022
Dimensions of cell H(mm) x h(mm)	32 x 2	850 x 24	210 x 145
Ra_h	10^7	4x10^{11}	1x10^{15}
Ra_H	5x10^{10}	2x10^{16}	3x10^{15}
Re_h	3	450	3700
Re_H	50	1.6x10^4	5500

Table 1. Table of parameters used in CFD validation cases.

Mesh Size	Eklund	Ziegler k-ε	Ziegler k-ω	Konishi
ΔY_{min} (mm)	0.06	0.48	0.16	0.01
ΔZ_{min} (mm)	0.02	4.25	2.125	0.4
ΔY_{max} (mm)	0.06	0.48	1	2.1
ΔZ_{max} (mm)	0.02	4.25	2.125	2.3

Table 2. Mesh sizes for each case, minimum (near wall) and maximum (middle cell) in Y and Z directions. The Ziegler k-ω model uses a finer near wall mesh than the Ziegler k-ε model (smaller ΔY_{min}).

CFD Model Validation and Discussion

Three cases are discussed, a small laboratory sized cell [3], a large typical industrial size [7] and a large very wide cell [6]. All three cases provide data which is used for comparison with the CFD model. The Rayleigh number (*Ra*) from Gurniki [5], and the Reynolds number (*Re*) are defined as follows:

$$Ra_h = \frac{g\beta \dot{m}_{copper} h^4}{\upsilon^2 D} \qquad Ra_H = \frac{g\beta \dot{m}_{copper} H^4}{\upsilon^2 D} \tag{7}$$

$$Re_h = \frac{hV}{\upsilon} \qquad Re_H = \frac{HV}{\upsilon} \tag{8}$$

where V (m s^{-1}) is velocity scale, h (m) and H (m) are the width and height of the system, respectively, ν (m^2 s^{-1}) is kinematic viscosity. These dimensionless numbers are provided in table 1 for each case, along with other important operating conditions.

Small Scale Laminar Case

This section compares the model with the small scale experiment of Eklund et al. [3, 4]. A fine uniform mesh (in both Y and Z) is used (see table 2), and the laminar CFD model is used since Re_h~1 and Ra_h=10^7 are low (see table 1). There is a very good agreement between the CFD results and experimental data in figure 2. In figure 2(a), both CFD results and experimental data indicate that near the cathode and anode there is downflow and upflow respectively, due to the deposition and removal of copper to and from the respective plate. The upflow and downflow occurs in the boundary layer where there is large concentration gradient (figure 2(c)), and the width of the boundary layer is predicted nicely compared to the data. CFD results (and experimental data) in figure 2 indicate that in a large portion of the middle of the cell there is very little flow. This is consistent with a natural convection recirculation zone, with the electrolyte moving downwards near the anode, and upwards near the cathode, due to the copper flux at each electrode. Copper stratification is clearly evident in the experimental data and the CFD prediction in figure 2(b), due to the lighter depleted copper electrolyte rising and the heavy metal laden electrolyte falling.

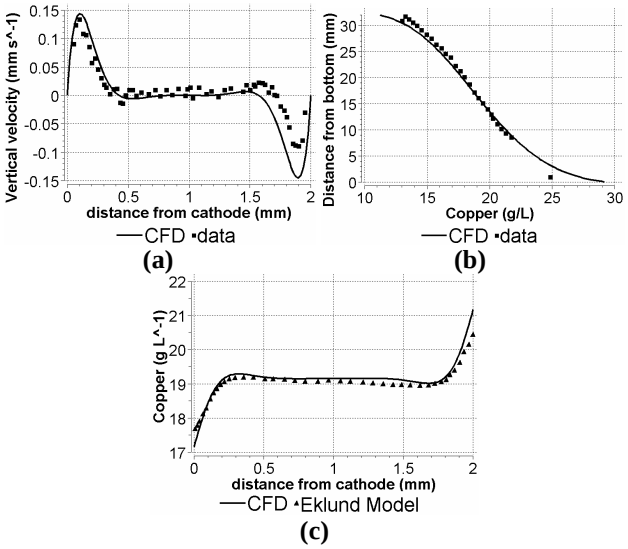

Figure 2. Comparison between CFD results (solid lines) and experimental data (squares) from [3] (a) vertical velocity component (mm s^{-1}) versus distance from cathode (mm) at mid cell height, (b) copper concentration (g L^{-1}) at a mid-cell width versus distance (mm) from base, (c) copper concentration (g L^{-1}) versus distance (mm) from cathode at mid cell height (triangles represent model predictions of Eklund et al. (1989)).

Large Scale Thin Case

This section shows the comparison of the model with experimental measurements of the vertical velocity of a large scale (thin) experiment from Ziegler [7]. The velocity is measured after 50 minutes has elapsed from start-up (figure 3 (symbols). A turbulence CFD model is used despite the transitional nature: Re_h~450 and Ra_h=4x10^{11} (see table 1). Figure 3 shows the comparison between the experimental and CFD results of the vertical velocity profile at cell mid-height, 425mm from the base. The steady state CFD model results are shown for two CFD models: k-ε with coarse wall mesh 50 by 200 cells (figure 3 dotted line), and k-ω with fine near wall mesh using 50 by 400 cells in Y and Z directions (figure 3 solid line). Both cases use a vertically uniform mesh (see table 2 for full mesh parameters). The two cases are compared because the k-ε (with coarse wall mesh) model was used by Gurniki [5], and we aim to determine the most appropriate numerical mesh and turbulence model. The predicted vertical velocity values for the k-ω model are in excellent agreement with the limited experimental data. The k-ε model comparison (figure 3 dotted line) is poor due to poor mesh resolution and k-ε model inaccuracy near the wall, resulting in a smearing of the velocity profile across the whole cross section.

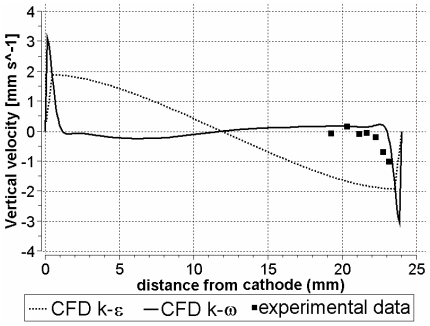

Figure 3. Comparison between CFD results k-ω with resolved wall mesh (solid lines) and k-ε with uniform mesh (dotted line) and experimental data (squares) from Ziegler [7]. Vertical velocity component (mm s^{-1}) versus distance from cathode (mm) at a height of 425mm from base.

In figure 4 we show details of the CFD results for the *k-ω* model (line plot of velocity shown in figure 3), with figure 4(a) showing a time snap shot of the contour plot of ratio of eddy to laminar viscosity, (b) the contours of the velocity scalar, (c) the vector plot and (d) the contour of the cadmium concentration. A natural convection recirculation zone is present, with the electrolyte moving downwards near the anode, and upwards near the cathode, due to the cadmium flux at each electrode. The electrolyte flow near the anode drags the highly metal-laden electrolyte downwards to the base, and the lighter metal-depleted electrolyte moves upwards near the cathode, causing a strong stratification in the cadmium concentration. In the middle of the cell, there is much slower flow, and small somewhat random fluctuations are present. Near the cathode and anode, there are small regions of high velocity (see figure 4(b)). The ratio of eddy to laminar viscosity in figure 4(a) is extremely low, indicating the turbulence level is insignificant; this suggests the system is not in the turbulent regime. Furthermore, the small vortexes in the middle of the geometry and the unsteady motion indicate the system is in the transitional regime. In figure 5 we show details of the CFD results for the *k-ε* model. This figure shows the poor description of the boundary layer (as also shown in figure 3), and dispersion of the boundary layer across the width of the gap, due to the smearing of the velocity profile by the *k-ε* model. The eddy viscosity remains high unlike in figure 4, for the *k-ω* model.

We can conclude the system is not turbulent but is in the transitional regime, based on the following: the low Reynolds number Re_h and the low Rayleigh number Ra_h, and the fact that the eddy viscosity becomes negligible with the experimentally validated *k-ω* model. We show in the next section that larger (wider) systems are more subject to turbulence, due to the extra width and space for eddies to develop.

Large Scale Wide Case

A large scale (wider) experiment by Konishi [6] has also been simulated, with a *k-ω* model and refined wall mesh (see table 2 for mesh parameters), in addition to a refined mesh at the top and bottom of the geometry. A turbulence model is appropriate due to the large Reynolds and Rayleigh numbers: Re_h~3700 and $Ra_h=1x10^{15}$ (see table 1). This case is large being 210mm tall and very wide (145mm), compared with the previous case from Ziegler [7] which was 24mm wide and 850mm tall. The CFD prediction shown in figure 6(a) and (b) is very good. Figures 7 and 8 show the CFD results, with figure 7 showing time snap shot of the velocity vector field and streamlines, and figure 8(a) showing the speed (log scale) and figure 8(b) the ratio of eddy and laminar viscosity. The streamlines with squares in figure 7 represent clockwise recirculation, and those with circles represent anti-clockwise recirculation. The large recirculation zone (circles) in the middle is where the ratio of eddy to laminar viscosity is high, and this is moving in the opposite direction to that expected, counter to the recirculation near the electrodes. This unexpected result is due to the clockwise recirculation near the cathode and anode plates (streamlines with circles) and the vortex at the top (squares), which drags electrolyte in the opposite direction with anticlockwise direction (circles).

The width of this Konishi [6] geometry is almost an order of magnitude larger than the Ziegler [7] case, and the eddy viscosity is now reasonably high, unlike the smaller (in width) Ziegler [7] case above (see figure 4), and this suggests the system is moderately turbulent. We can conclude that the width is a more important length scale than the height from the point of view of onset of turbulence, due to the fact that the eddies are restricted in the smaller gap width, and are free to evolve and move around in the larger scale system.

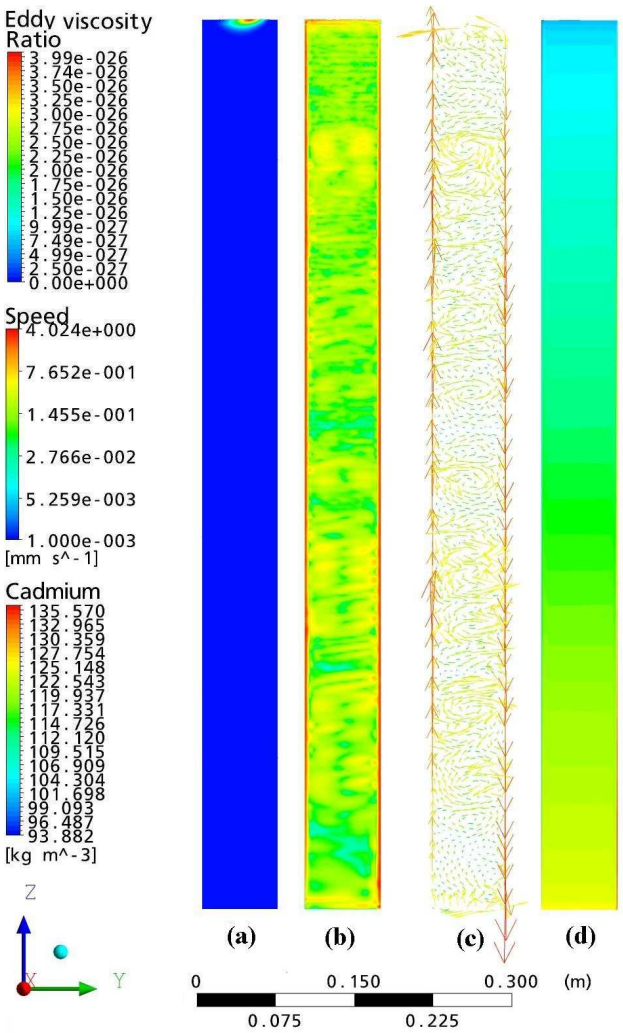

Figure 4. CFD results used to compare with Ziegler [7] for *k-ω* model, (a) contour plot of ratio of eddy to laminar viscosity (-) (b) contour plot of speed scalar (log scale) (mm s^{-1}), (c) velocity vectors coloured by speed (log scale), and (d) contour plot of cadmium concentration (kg m^{-3}). Horizontal scale increased by a factor of 3 to view results.

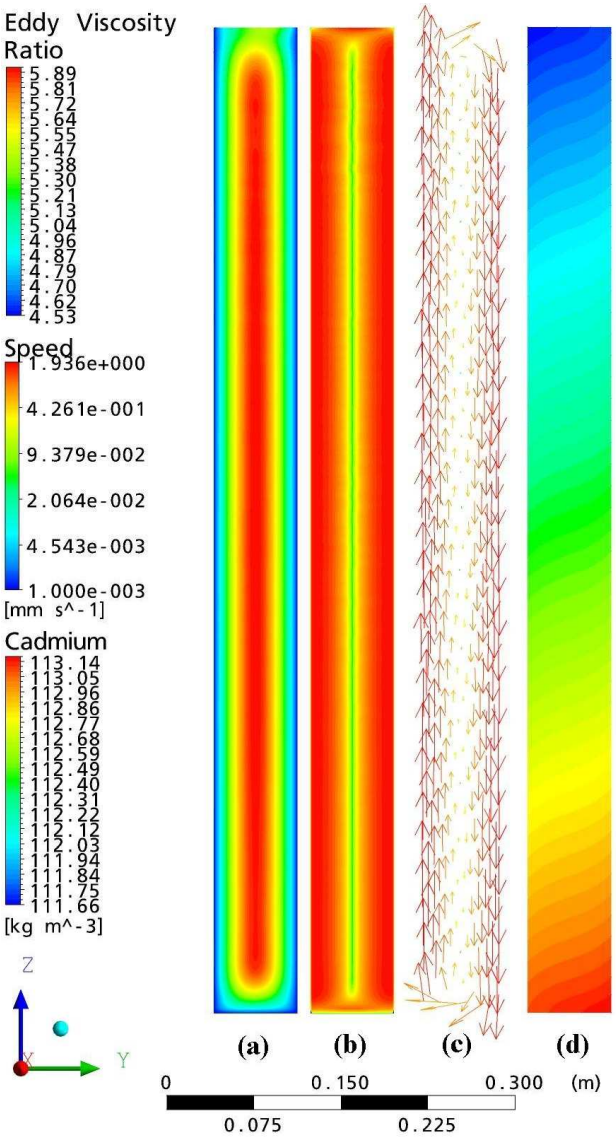

Figure 5. CFD results used to compared with Ziegler [7] for k-ε model, (a) contour plot of ratio of eddy to laminar viscosity (-) (b) contour plot of speed scalar (log scale) (mm s^{-1}), (c) velocity vectors coloured by speed (log scale), and (d) contour plot of cadmium concentration (kg m^{-3}). Horizontal scale increased by a factor of 3 to view results.

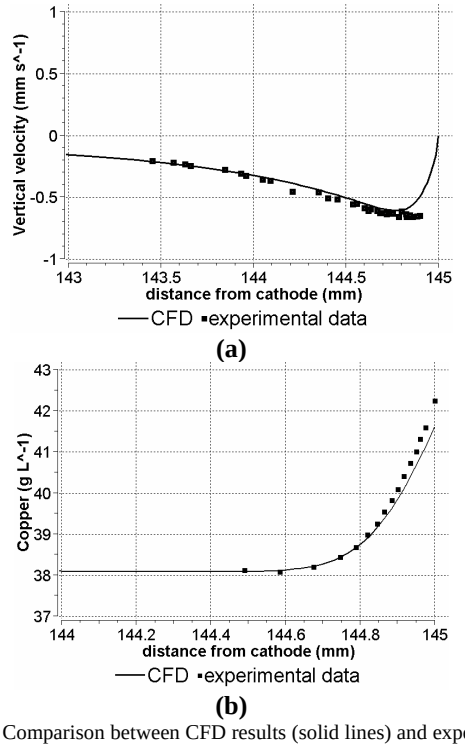

Figure 6. Comparison between CFD results (solid lines) and experimental data (squares) from Konishi [6]. (a) Vertical velocity component (mm s^{-1}) versus distance from cathode (mm) and (b) copper concentration (mm s^{-1}) versus distance from cathode (mm) at a height of 140mm from base.

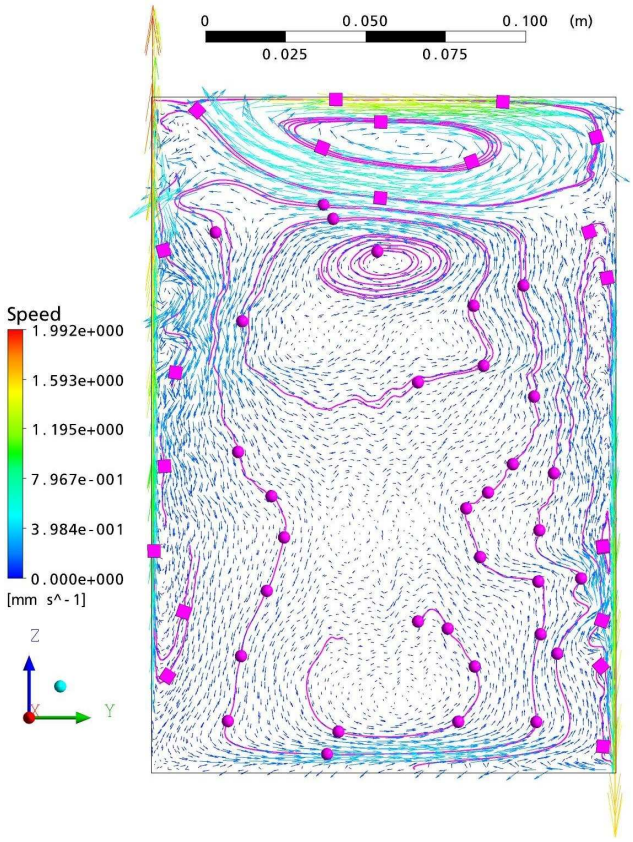

Figure 7. CFD results used to compare with Konishi [6], vector field coloured by speed and pink streamlines (squares – clockwise recirculation zone, circles - anti-clockwise recirculation zone).

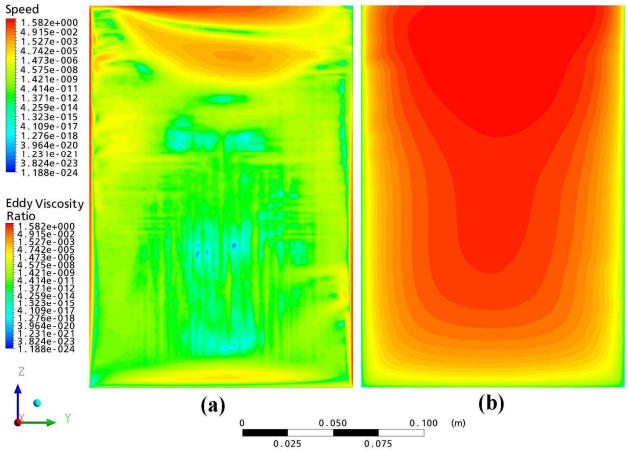

Figure 8. CFD results used to compare with Konishi [6], (a) contour plot of speed scalar (log scale) and (b) contour plot of ratio of eddy viscosity to laminar viscosity (-).

Conclusions

A CFD model for ER has been developed and compared to several different sized experimental systems from the literature. The CFD results compared very well with the small scale experimental data, and were also very good for the larger scale experiments of Ziegler [7] and Konishi [6]. The k-ε model on a coarse wall mesh is unsatisfactory in comparison to the k-ω model with a fine mesh near the wall. The CFD model predicted unsteady behaviour for the experiment in [7]. The larger gap width (145mm) case in [6] led to a more unstable but not turbulent system, with eddies forming and moving into large eddies away from the electrodes. The width of the system has more of an effect on onset of turbulence rather than the height.

Acknowledgments

The authors gratefully acknowledge Mike Horne, Peter Witt, Darrin Stephens and Mike Nicol for helpful discussions. AMIRA P705A sponsors are acknowledged for permission to publish.

References

[1] ANSYS, (2007), CFX-11 Solver, ANSYS Inc., Canonsburg, USA, website address www.ansys.com/cfx

[2] Denpo, K., Teruta, S., Fukunaka, Y. and Kondo, Y., 1983, Turbulent natural convection along a vertical electrode, *Metallurgical Transactions B*, 14B, 633-643.

[3] Eklund, A., Alavyoon, F., Simonsson, D., Karlsson, R. and Bark, F. 1991. Theoretical and experimental studies of free convection and stratification of electrolyte in a copper refining cell, *Electrochemica Acta*, 36 (8), 1345-1254.

[4] Eklund, A., Simonsson, D., Alavyoon, F., Karlsson, R., and Bark, F. 1991. Theoretical and experimental studies of free convection in a copper refining cell, *I. Chem. E. Symposium Series No 112*, 112, 47-58.

[5] Gurniki, F. Bark, F. and Zahari, S., 1999. Turbulent free convection in large electrochemical cells with a binary electrolyte, *J. Appl. Electrochem.*, 29, 27-34.

[6] Konishi, Y., Tanaka, Y. Kondo, Y. and Fukunaka, Y., 2000. Copper dissolution phenomena along a vertical plane anode in CuSO4 solution. *Electrochemica Acta*, 46, 681-690.

[7] Ziegler, D. and Evans, J., 1986. Mathematical modelling of electrolyte circulation in cells with planar vertical electrodes: I electrorefining cells. *J. Electrochemical Soc.*, 133 (3), 559-566.